

Received 29 May 2023, accepted 5 July 2023, date of publication 10 July 2023, date of current version 14 July 2023.

Digital Object Identifier 10.1109/ACCESS.2023.3293656

RESEARCH ARTICLE

Intelligent Dynamic Collision Avoidance Strategy of Hydrogen Fuel Cell Unmanned Ship via Improved Fusion Dynamic Window Method

ZIMIN WANG 

International College, Wuhan University of Science and Technology, Wuhan 430065, China

e-mail: ZiminwangDE@163.com

This work was supported by the Wuhan University of Science and Technology International Talent Fund Project under Grant 2023J0503.

ABSTRACT In this study, a novel fusion dynamic window method is proposed. The safety field obstacle model of obstacle ships is explored to improve the obstacle collection of speed obstacle method, so that the collision avoidance process of Hydrogen Fuel Cell Unmanned Ship (HFCUS) can retain more feasible paths. The speed window is discretized, and the speed vector space is filtered based on the speed obstacle collection in the safety field to realize the fusion of algorithms. The objective evaluation function is improved, and the rule constraint function is presented, so that the collision avoidance behavior of HFCUSs conforms to the constraints of the Convention on the International Regulations for Preventing Collisions (COLREGS), and the safety in the collision avoidance process is improved. Simulation and experiment are verified that the proposed algorithm can effectively avoid dynamic obstacle ships, and the avoidance behavior meets the rules and constraints. HFCUS is realized the safe navigation in the environment of dynamic obstacle ships.


INDEX TERMS Dynamic collision avoidance, hydrogen fuel cell unmanned ship (HFCUS), obstacle ships, fusion dynamic window method, speed barrier method.

I. INTRODUCTION

In order to reduce the environmental problems that arise due to the need for electrical energy triggered by the increasing population in the world, and in line with sustainable development, more environmentally friendly energy sources are being researched instead of fossil fuels [1]. With the rapid development of science and technology, the amount of fuel being used is gradually increasing. The International Energy Agency (IEA) Energy Efficiency Market Report indicated that coal, natural gas, petroleum, and other fossil fuels account for over 85% of the world's total energy consumption. Currently, most of the energy used by fossil energy is converted from the accumulation of solar energy over the earth. The requirements for green energy have become more critical with the increasing risk from the global warming effect. The Proton Exchange Membrane Fuel Cells (PEMFC) are widely used on vehicles. In the process of massive using

this energy, it can cause more pollution and hazards, such as air pollution, acid-rain, Greenhouse effect, and so on. For the rising environmental protection concerns, many developed countries are actively contributing to research and development of low-pollution renewable energy sources, such as fuel cells, wind power generation, solar cells, and hydrogen; in terms of clean energy, fuel cells may be one of the best choices [2].

Considering the disadvantages and advantages of fuel cells in a holistic framework, compared to diesel engines, gas turbine generators and wind turbines; fuel cells have a higher capital cost with 1500-3000\$/kW. There are difficulties and limitations associated with the use of fuel cells. The requirement for very high purity of the hydrogen fuel used, low power density per volume, the short lifetime of fuel cells, and low durability are found in the literature as limitations [3]. A hydrogen fuel cell has many advantages, such as no pollution, high efficiency, low noise and continuous operation. Therefore, it has the potential to be widely applied in both the power propulsion and power supply of a ship [4].

The associate editor coordinating the review of this manuscript and approving it for publication was Sotirios Goudos .

Autonomous Surface Vehicles (ASVs) are becoming consolidated robotic tools for marine, coastal and inland surveys. ASVs are usually equipped with electronic instruments to perform autonomous geo-morphological, biological, chemical, and physical analyses, as well as data collection. Autonomous Unmanned Surface Vehicles (USVs), also known as unmanned surface ships or (in some cases) as autonomous surface vehicles (ASVs), are boats that operate on the surface of the water unmanned [5]. Improving the sub-sea endurance and the power system efficiency of unmanned underwater vehicles (UUVs) has become more important in recent years as their growing demands in different applications. Integrated electric power systems are commonly applied in UUVs with different types of batteries as power sources. Utilizing fuel cells hybridized with batteries is one of the most efficient ways to increase the UUV's range and overall system efficiency. In 2023, a conceptual design was presented for fuel cell/battery hybrid UUV. To elaborate on the design process, the UUV fuel cell stacks, the commercial fuel cell UUVs, the technologies of the fuel and oxidant storage, and the electrical energy storage subsystems are reviewed. Also, analytical investigations have been presented on the degree of hybridization (DOH) between fuel cells and batteries. The fuel cell/battery hybrid system for UUV is designed and the technologies of its main components are proposed as the final step of the conceptual design process [6].

This study uses the world's first hydrogen fuel cell passenger vessel 'FCS Alsterwasser' as a case study. This vessel was developed as part of the ZEMSHIPS project funded by the EU-Life program. A hydrogen filling station has been built by Linde Group as a part of this project. FCS Alsterwasser operates around Hamburg, Germany on Lake Alster, HafenCity, the River Elbe and the inner city waterways for round and charter trips [7], [8]. The FCS Alsterwasser is shown in Figure 1.



FIGURE 1. The world's first hydrogen fuel cell passenger vessel 'FCS Alsterwasser' [7].

The shape of Hydrogen Fuel Cell Unmanned Ship (HFCUS) is shown in Figure 2. The safe design principles and leakage risks of the hydrogen gas supply system of China's first newbuilt hydrogen-powered ship has been examined. The computational fluid dynamics tool FLACS has been



FIGURE 2. The shape of hydrogen fuel cell unmanned ship (HFCUS).

utilised to analyse the hydrogen dispersion behaviour and concentration distributions in the hydrogen fuel cell room based on the ship's parameters [9].

As for unmanned surface vessels (USVs), the path planning and tracking are essential technologies. However, the kinodynamic constraints and actuator faults bring difficulties in finding feasible paths and control efforts. In 2023, a collision avoidance strategy has been proposed for USV by developing the kinodynamic rapidly exploring random tree-smart (kinodynamic RRT*-smart) algorithm and the fault-tolerant control method. The kinodynamic RRT*-smart shows its advantages in terms of path length, cost and running time by utilizing the triangular inequality and the intelligent biased sampling strategy. A feasible and collision-free trajectory can be provided consideration of kinodynamic constraints [10]. With respect to navigation practices and real-ship applications, a stable and reliable technical program for automatic ship navigation was provided. An improved route-plan-guided artificial potential field (APF) method was presented by balancing the attractive and repulsive forces, resolving the irrationality and swaying of the collision avoidance (CA) strategy, and extending the applicability of the International Regulations for Preventing Collisions at Sea (COLREGS) [11]. In complex scenarios full of reciprocal obstacles, selecting the optimal agent velocity, the challenge of solving the collision avoidance path planning problem lies in adaptively. To achieve autonomous collision avoidance for unmanned surface vehicles (USVs), a distributed multi-USVs navigation method based on deep reinforcement learning (DRL) was proposed in 2023, which solved the collision avoidance path planning problem with limited information by combining the concept of reciprocal velocity obstacle (RVO) with a DRL scheme to [12].

In addition, based on fuzzy C-means clustering and ant colony optimization algorithms, a heterogeneous UAV multi-task redistribution coordination problem with target priority constraint was proposed. According to the corresponding task reassignment strategy, the dynamic redistribution model of multi-UAV mission under the dynamic emergency adjustment scenario can obtain better performance to complete the corresponding tasks. The developed graphical modeling

and analysis software platform is deployed to realize the dynamic redistribution model of multiple UAV tasks under dynamic surge scenes, and the effectiveness and reliability of the proposed task reassignment model are verified [13], [14].

Based on the above literatures, this study proposes a novel fusion dynamic window method. The speed window is discretized, and the speed vector space is filtered based on the speed obstacle collection in the safety field to realize the fusion of algorithms. The objective evaluation function is improved, and the rule constraint function is presented, so that the collision avoidance behavior of hydrogen fuel cell unmanned ships conforms to the constraints of the COLREGS Convention and improves the safety in the collision avoidance process. The simulation is verified that the proposed algorithm can effectively avoid dynamic obstacle ships, and the avoidance behavior meets the rules and constraints, so as to realize the safe navigation of hydrogen fuel cell unmanned ships in the environment of dynamic obstacle ships.

The rest of this paper is organized as follows. Improved speed barrier method based on the field of safety, model description of the speed barrier method, and improved collision model calculation for speed obstacle method are introduced in Section II. Section III proposes collision avoidance planning based on improved speed obstacle fusion dynamic window method, including discretization of velocity window, trajectory prediction combined with dynamic window method and merging the evaluation function of the dynamic window method. The dynamic collision avoidance simulation and result analysis and verification are illustrated in Section IV. The experimental results are shown as well. Finally, the conclusion is given in Section V.

II. IMPROVED SPEED BARRIER METHOD BASED ON THE FIELD OF SAFETY

A. MODEL DESCRIPTION OF THE SPEED BARRIER METHOD

The speed obstacle theory is to transform the collision avoidance planning of hydrogen fuel cell unmanned ships to obstacle ships into the study of the speed space of the unmanned ships themselves, and it uses the relative position and relative speed vector difference between hydrogen fuel cell unmanned ships and obstacle ships to construct a triangular region representing the collision threat, that is, the set of speed obstacles. As shown in Figure 3(a), it represents a system space composed of a hydrogen fuel cell unmanned ship and an obstacle ship at a certain time, where A represents the hydrogen fuel cell unmanned ship, B represents the obstacle ship, and the speeds of A and B are V_A and V_B , respectively. Expand the model of A and B into a circle representing the respective barrier domains, where the radius of the barrier domains of A and B is R_A and R_B , respectively.

In order to obtain the velocity barrier space, the velocity vector of B is mapped to the configuration space of A, and the radius of A is superimposed on B, so that A can be abstracted

into a particle, and the radius of B expands to $R' = R_A + R_B$, to obtain a new obstacle threshold O_A and O_B . The relative velocity of A and B is expressed in $V_{A,B}$, i.e. $V_{A,B} = V_A - V_B$. Define a ray λ_{AB} drawn from the center of a hydrogen fuel cell unmanned ship in the direction of relative velocity:

$$\lambda_{AB}(A, V_{A,B}) = \{A + V_{A,B}t \mid t \geq 0\} \quad (1)$$

here, the end of the ray λ_{AB} represents the relative position that the hydrogen fuel cell unmanned ship can reach after the t moment, when the hydrogen fuel cell unmanned ship and the obstacle ship maintain the original sailing state. When the end of the ray λ_{AB} falls within the O_B surrounding the obstacle domain, the hydrogen fuel cell unmanned ship collides with the obstacle ship. Defining the set of all relative velocity $V_{A,B}$ that could cause A to collide with B is $CC_{A,B}$, which represents the set of velocity obstacles, and $CC_{A,B}$ can be represented as shown in equation (2):

$$CC_{A,B} = \{V_{A,B} \mid \lambda_{AB}(A, V_{A,B}) \cap O_B \neq \emptyset\} \quad (2)$$

It can be observed that the set of speed obstacles is a triangle with A as the apex and two tangent lines LF and LR bounded by A to the obstacle domain O_B , and that all relative velocity $V_{A,B}$ falling within the obstacle zone $CC_{A,B}$ will cause A and B to collide while B maintains the original sailing state, and the relative velocity falling outside the obstacle zone $CC_{A,B}$ will not cause A and B to collide. Due to the inconvenience of the expression of the relative velocity $V_{A,B}$, consider converting the speed obstacle set $CC_{A,B}$ into the reference space with the absolute speed of the hydrogen fuel cell unmanned ship as the reference, that is, summing all the velocities and V_B in the $CC_{A,B}$ to obtain the speed obstacle set VO at absolute speed:

$$VO = CC_{A,B} \oplus V_B \quad (3)$$

where \oplus represents Minkowski vector addition, the meaning of which is to add the velocity V_B each relative velocity in the $CC_{A,B}$, at this time, if the hydrogen fuel cell unmanned ship velocity vector V_A falls in the speed barrier set VO , then there is a danger of collision between the two; Conversely, hydrogen fuel cell unmanned ships have no risk of collision. Figure 3(b) shows the spatial schematic of the speed barrier system composed of A and B.

B. IMPROVED SPEED OBSTACLE METHOD COLLISION AVOIDANCE PLANNING BASED ON SAFETY FIELD

Generally, in the case of a large difference between the length and width of the obstacle ship, the expansion of the collision avoidance threshold of the obstacle ship into a circle in the traditional speed obstacle method will make the hydrogen fuel cell unmanned ship lose more feasible path points, and it is not conducive to the search for the optimal collision avoidance path, so it is considered that the circular expansion model in the speed obstacle method will be replaced by a safety domain model that is more in line with the actual shape of the obstacle ship. At this time, the system space consisting of a hydrogen fuel cell unmanned ship and an obstacle ship

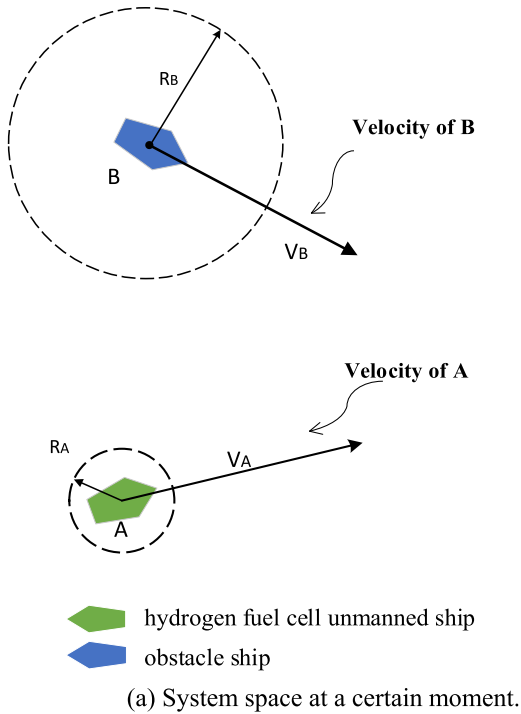


FIGURE 3. Schematic diagram of traditional speed barriers.

can be shown in Figure 4(a). It is still considered that the A model is expanded into a circle with a radius of R_A , while the obstacle ship B model is replaced with a safety domain model that is more in line with the hull, where the major and minor axes of the obstacle ellipse of the B model are mL and nL , respectively. Abstracting A into a particle, the major and minor axes of B expand by a R_A length to obtain a new barrier threshold O_B . Similarly, the set of velocity obstacles with A as the vertex and tangents LF and LR as the boundary CCA,B

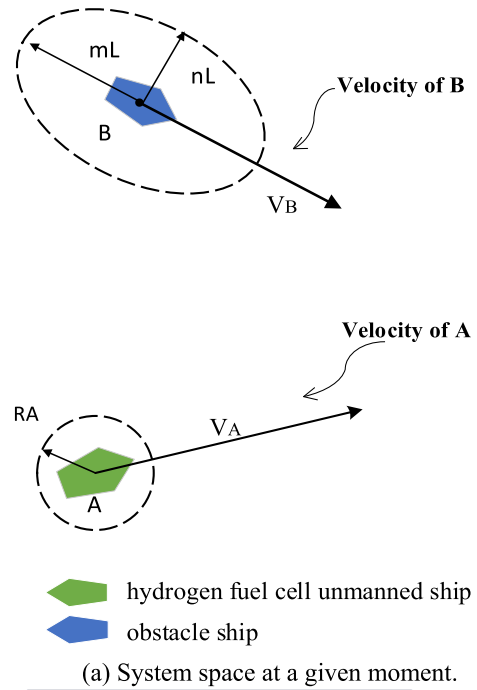


FIGURE 4. Schematic diagram of speed barriers based on safety fields.

and the set of velocity obstacles at absolute velocity VO are obtained, as shown in Figure 4(b).

It is worth noting that compared with the obstacle threshold enclosing circle, the obstacle ship safety domain model has more concept of “direction”, which makes the boundary LF and LR of the speed obstacle set based on the safety field change in different directions, resulting in the size of the obstacle area will also change. The biggest advantage of this treatment method is that the hydrogen fuel cell unmanned ship can adaptively adjust the size of the speed obstacle set

according to the different directions of the obstacle ship, so as to reduce the loss of feasible path points and obtain a better collision avoidance path.

C. IMPROVED COLLISION MODEL CALCULATION FOR SPEED OBSTACLE METHOD

Based on the speed obstacle theory, the collision relationship between the hydrogen fuel cell unmanned ship and the obstacle ship is analyzed. The mathematical collision model of hydrogen fuel cell unmanned ship is shown in Figure 5, point $A(x_0, y_0)$ is the central position of hydrogen fuel cell unmanned ship, point $B(x_b, y_b)$ is the center of the obstacle ship safety field model, the speed of the hydrogen fuel cell unmanned ship is set to V_A , the heading angle is α , the speed of the obstacle ship is V_B , the heading angle β , the relative speed of the two can be expressed by $\Delta V = V_A - V_B$, and the relative speed heading angle is ψ . The angle between point A of the center of the hydrogen fuel cell unmanned ship and the center of the obstacle ship B is θ , the angle between the relative velocity ΔV and the connection AB is γ , representing the azimuth of the hydrogen fuel cell unmanned ship, the V_S and V_θ are the two velocity components of the parallel and vertical connection AB of ΔV , and the AC_1 and AC_2 are the two tangents in the safety field, where $\angle BAC_1$ and $\angle BAC_2$ represent the collision safety angle μ . A schematic diagram of the mathematical collision model of the hydrogen fuel cell unmanned ship is shown in Figure 5.

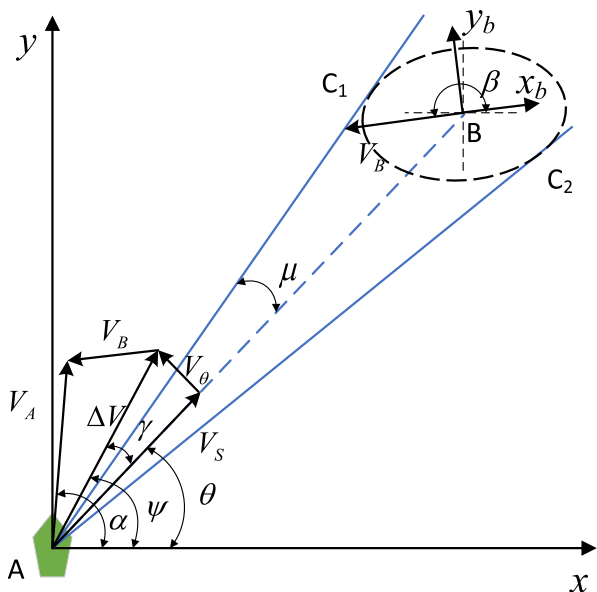


FIGURE 5. Schematic diagram of the mathematical collision model of hydrogen fuel cell unmanned ship.

(i) Collision safety corner μ

The obstacle ship coordinate reference system $x_b - B - y_b$ is established with the obstacle ship as the center, and the standard equation of the safety domain model of the obstacle

ship can be expressed as:

$$\frac{x^2}{a^2} + \frac{y^2}{b^2} = 1 \tag{4}$$

where $a = mL + R_A$ represents the major axis and $b = nL + R_A$ represents the minor axis. Considering the conversion of the coordinates of point A in the center of the hydrogen fuel cell unmanned ship to the coordinates of the obstacle ship, then the coordinates of point A, $[x'_0, y'_0]^T$ under $x_b - B - y_b$ can be obtained from equation (5):

$$[x'_0, y'_0]^T = \begin{bmatrix} \cos\beta & \sin\beta \\ -\sin\beta & \cos\beta \end{bmatrix}^{-1} \left(\begin{bmatrix} x_0 \\ y_0 \end{bmatrix} - \begin{bmatrix} x_b \\ y_b \end{bmatrix} \right) \tag{5}$$

Let the tangent AC_1 and AC_2 tangent to the point of the ellipse C_1C_2 coordinates are $(x_i, y_i), i = 1, 2$, then the standard equation and tangent equation of the simultaneous domain model are solved by equation (5) to solve the coordinates of tangent point $(x_i, y_i), i = 1, 2$:

$$\begin{cases} \frac{x_i^2}{a^2} + \frac{y_i^2}{b^2} = 1 \\ \frac{x_i x'_0}{a^2} + \frac{y_i y'_0}{b^2} = 1 \end{cases} \tag{6}$$

Get the coordinates of the tangent point $(x_i, y_i), i = 1, 2$, and you can get the slopes k_1 and k_2 of the tangents AC_1 and AC_2 :

$$k_1 = \frac{y_1 - y'_0}{x_1 - x'_0}, k_2 = \frac{y_2 - y'_0}{x_2 - x'_0} \tag{7}$$

At this time, the angle between the tangents AC_1 and AC_2 can be obtained from the slopes k_1 and k_2 , and the collision safety angle μ is half of the angle between the tangents, which can be expressed as shown in equation (8):

$$\mu = \frac{1}{2} \arctan \left(\frac{|k_1 - k_2|}{(1 + k_1 k_2)} \right) \tag{8}$$

(ii) Hydrogen fuel cell unmanned ship azimuth γ

According to the velocity vector trigonometry, the velocity components of V_S and V_θ can be expressed as equation (9):

$$\begin{cases} V_S = V_A \cos(\alpha - \theta) - V_B \cos(\beta - \theta) \\ V_\theta = V_A \sin(\alpha - \theta) - V_B \sin(\beta - \theta) \end{cases} \tag{9}$$

The angle between the relative velocity ΔV and the line AB can be calculated from equation (9), which is the azimuth angle, as shown in equation (10):

$$\begin{aligned} \gamma &= \frac{V_\theta}{V_S} = \arctan \left(\frac{V_A \sin(\alpha - \theta) - V_B \sin(\beta - \theta)}{V_A \cos(\alpha - \theta) - V_B \cos(\beta - \theta)} \right) \\ &= f(V_A, V_B, \alpha, \theta) \end{aligned} \tag{10}$$

(iii) Collision avoidance adjustment strategy for hydrogen fuel cell unmanned ships

Combined with the relative velocity ΔV , by comparing the collision safety angle μ with the azimuth angle γ , it can be judged whether there is a collision risk. If $|\gamma| > \mu$, the hydrogen fuel cell unmanned ship does not need to adjust its own motion state; otherwise, there is a collision risk. The battery unmanned ship needs to adjust its course and speed to avoid collision.

It can be seen from equation (10) that γ is a function of the speed and heading of the hydrogen fuel cell unmanned ship and the obstacle ship, and the derivative of both sides of the function can be obtained:

$$d\gamma = \frac{1}{1+f^2}df \quad (11)$$

$$\frac{1}{1+f^2} = \frac{V_B \cos(\beta - \theta) - V_A \cos(\alpha - \theta)}{V_A^2 + V_B^2 - 2V_A V_B \cos(\alpha - \beta)} \quad (12)$$

$$df = \frac{\partial f}{\partial V_A} dV_A + \frac{\partial f}{\partial V_B} dV_B + \frac{\partial f}{\partial \alpha} d\alpha + \frac{\partial f}{\partial \beta} d\beta \quad (13)$$

Since the hydrogen fuel cell unmanned ship can only adjust its own motion state, but cannot change the motion of the obstacle ship, considering that the movement of the obstacle ship changes very little in a short time interval, it can be assumed that $dV_B = 0$, $d\beta = 0$, equation (13) can be approximated as:

$$df = \frac{\partial f}{\partial V_A} dV_A + \frac{\partial f}{\partial \alpha} d\alpha \quad (14)$$

here,

$$\frac{\partial f}{\partial V_A} dV_A = \frac{-V_B \sin(\alpha - \beta)}{[V_A^2 + V_B^2 - 2V_A V_B \cos(\alpha - \beta)]^2} \quad (15)$$

$$\frac{\partial f}{\partial \alpha} d\alpha = \frac{V_A [V_A - V_B \cos(\alpha - \beta)]}{[V_A^2 + V_B^2 - 2V_A V_B \cos(\alpha - \beta)]^2} \quad (16)$$

At this time, equation (11) can be expressed in differential form as:

$$\Delta\gamma = \frac{V_B \sin(\beta - \alpha)}{V_A^2 + V_B^2 - 2V_A V_B \cos(\beta - \alpha)} \Delta V_A + \frac{V_A - V_A V_B \cos(\alpha - \beta)}{V_A^2 + V_B^2 - 2V_A V_B \cos(\beta - \alpha)} \Delta \alpha \quad (17)$$

It can be seen from equation (17) that $\Delta\gamma$ is closely related to the speed and course of the hydrogen fuel cell unmanned ship. This equation can be used to calculate the adjusted speed and course range of the hydrogen fuel cell unmanned ship under the requirements of collision avoidance. If $|\gamma| \leq \mu$, the hydrogen fuel cell unmanned ship needs to change its course or speed to avoid collision. The adjustment range is $\Delta\gamma > \mu - \gamma$ or $\Delta\gamma < -\mu - \gamma$. The specific adjustment strategy needs to be determined in combination with the navigation rules in different scenarios.

III. COLLISION AVOIDANCE PLANNING BASED ON IMPROVED SPEED OBSTACLE FUSION DYNAMIC WINDOW METHOD

A. DISCRETIZATION OF VELOCITY WINDOW

During the movement of the hydrogen fuel cell unmanned ship, if the combination of a set of linear velocity and angular velocity within the next time interval Δt is given, the trajectory point that the hydrogen fuel cell unmanned ship can

travel to within Δt can be predicted. Considering the mechanical properties of the hydrogen fuel cell unmanned ship, there are limitations on its maximum speed u_{max} and maximum acceleration \dot{u}_{max} , maximum angular velocity r_{max} and maximum angular acceleration \dot{r}_{max} , so the hydrogen fuel cell unmanned ship can be given within the time interval Δt . The combination of linear velocity and angular velocity of the ship is limited, and these velocity combinations (u, r) constitute the velocity space of the hydrogen fuel cell unmanned ship. Using these velocity combinations, the hydrogen fuel cell unmanned ship within Δt can be calculated. The collection of possible trajectory spaces constitutes a navigation area accessible to the hydrogen fuel cell unmanned ship. The hydrogen fuel cell unmanned ship searches the accessible navigation area and selects the required trajectory through the designed trajectory evaluation function.

When designing the speed window of the hydrogen fuel cell unmanned ship, it is necessary to consider the limitations of the maximum moving speed (u_{max}, r_{max}) and maximum acceleration $(\dot{u}_{max}, \dot{r}_{max})$. Considering the mechanical properties of the hydrogen fuel cell unmanned ship, the velocity and angular velocity variables (u, r) are constrained in combination with the maximum velocity and maximum angular velocity that it can achieve, as shown in equation (18):

$$V_s = \left\{ (u_s, r_s) \mid \begin{array}{l} u_s \in [0, u_{max}] \\ r_s \in [-r_{max}, r_{max}] \end{array} \right\} \quad (18)$$

Considering that the hydrogen fuel cell unmanned ship will be constrained by the maximum power during navigation, there is a limitation on the acceleration and deceleration of the hydrogen fuel cell unmanned ship within Δt , so the hydrogen fuel cell unmanned ship is based on the current sailing speed during this period, The speed range V_d that can be obtained through acceleration and deceleration is as follows:

$$V_d = \left\{ (u_d, r_d) \mid \begin{array}{l} u_d \in [u + \dot{u}_{min} \Delta t, u + \dot{u}_{max} \Delta t] \\ r_d \in [r - \dot{r}_{max} \Delta t, r + \dot{r}_{max} \Delta t] \end{array} \right\} \quad (19)$$

In the equation, u and r represent the current speed and angular velocity of the hydrogen fuel cell unmanned ship, \dot{u}_{min} and \dot{u}_{max} are the minimum and maximum acceleration respectively, and \dot{r}_{max} is the maximum angular acceleration.

After the above speed range limitation operation, two speed ranges can be obtained, and their intersection is the speed range that can be obtained in the current state of the hydrogen fuel cell unmanned ship:

$$V_r = V_s \cap V_d \quad (20)$$

However, the speed of the hydrogen fuel cell unmanned ship in the set is continuous, which is not conducive to the sampling analysis of the step length iteration of the hydrogen fuel cell unmanned ship. Therefore, it is considered to discretize the reachable speed range set of the hydrogen fuel

cell unmanned ship, as shown in Figure 6. The speed set V_r is discretized, where u_{max} is discretized into M speed segments of the same size, $(-r_{max}, r_{max})$ is discretized into N direction segments of the same size, and the speed set V_r can be discretized into $M \times N$ velocity vectors (u_i, r_i) representing the magnitude and direction of the velocity. These discrete velocity vectors (u_i, r_i) constitute the velocity vector (Reachable Velocity, RV) that the hydrogen fuel cell unmanned ship can reach within Δt .

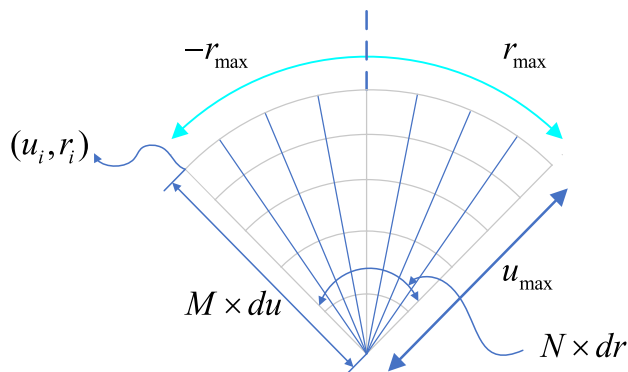


FIGURE 6. Discretized reachable velocity vector set RV.

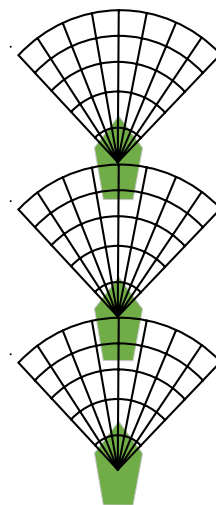
B. TRAJECTORY PREDICTION COMBINED WITH DYNAMIC WINDOW METHOD

After obtaining the speed vector set RV that the hydrogen fuel cell unmanned ship can reach, the trajectory prediction within a given time period can be generated for each set of speeds. For a given set of velocities (u_i, r_i) , define the prediction time period as t , if you want to get the trajectory of the hydrogen fuel cell unmanned ship within this period, you need to set a very small time increment Δt . In this way, a time series $[0, \Delta t, 2\Delta t, \dots, t]$ can be obtained.

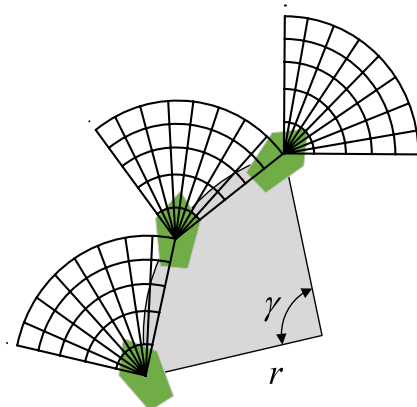
Usually, the prediction of the trajectory of the hydrogen fuel cell unmanned ship will be considered from two perspectives: (i) The hydrogen fuel cell unmanned ship does not perform steering movements, and the future trajectory of the hydrogen fuel cell unmanned ship is regarded as is a straight line, as shown in Figure 7(a); (ii) the hydrogen fuel cell unmanned ship keeps the linear velocity and angular velocity constant, as shown in Figure 7(b), at this time the future trajectory of the hydrogen fuel cell unmanned ship will be is a curve. The following two models of trajectory prediction are analyzed in detail:

For the situation in Figure 7(a), the surface hydrogen fuel cell unmanned ship is considered the forward motion and ignores the steering motion. Assuming that the current position and attitude of the hydrogen fuel cell unmanned ship are (x_0, y_0, θ_0) , and the velocity and angular velocity are (u_i, r_i) , then within a certain time interval Δt , the predicted trajectory of the hydrogen fuel cell unmanned ship can be shown in the

jectory



(a) The hydrogen fuel cell unmanned ship moves along a straight line.



(b) The hydrogen fuel cell unmanned ship moves in a curve.

FIGURE 7. Trajectory prediction model.

following equation (21):

$$\begin{cases} x_1 = x_0 + u_i \times \Delta t \cos(\theta_0) \\ y_1 = y_0 + u_i \times \Delta t \sin(\theta_0) \\ \theta_1 = \theta_0 \end{cases} \quad (21)$$

For the situation in Figure 7(b), when the surface hydrogen fuel cell unmanned ship keeps the linear velocity and angular velocity constant, the trajectory of the hydrogen fuel cell unmanned ship is presented a circular arc, and this predicted trajectory is more accurate. The operation of the hydrogen fuel cell unmanned ship is conformed to the actual situation. For a given current pose (x_0, y_0, θ_0) and velocity (u_i, r_i) of the hydrogen fuel cell unmanned ship, the predicted trajectory of the hydrogen fuel cell unmanned ship can be regarded as a

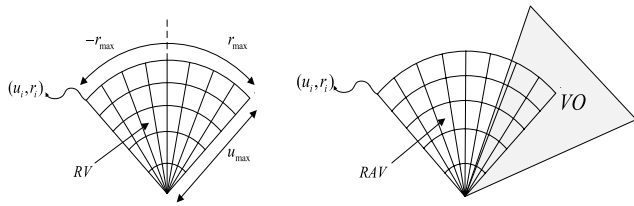


FIGURE 8. RV speed set and RAV speed set.

segment with an arc with radius $R' = |u/r|$. Within a certain time interval Δt , the predicted trajectory of the hydrogen fuel cell unmanned ship is shown in equation (22):

$$\begin{cases} x_1 = x_0 - \frac{u_i}{r_i} \sin(\theta_0) + \frac{u_i}{r_i} \sin(\theta_0 + r_i \Delta t) \\ y_1 = y_0 - \frac{u_i}{r_i} \cos(\theta_0) - \frac{u_i}{r_i} \cos(\theta_0 + r_i \Delta t) \\ \theta_1 = \theta_0 + r_i \Delta t \end{cases} \quad (r_i \neq 0) \quad (22)$$

In fact, the case where the predicted trajectory of the hydrogen fuel cell unmanned ship is a straight line is essentially a special state of the predicted trajectory is a circular arc, that is, when r_i in equation (22) satisfies $r_i = 0$, equation (22) will be changed into the form of equation (20), at this time the predicted trajectory of the hydrogen fuel cell unmanned ship becomes a straight line.

The RV set is the speed space that the hydrogen fuel cell unmanned ship can reach within a certain time interval, and the speed space in the VO is the speed vector set of the hydrogen fuel cell unmanned ship that has the risk of collision in the future. Combined with the speed obstacle set, it can be filtered the RV set, as shown in Figure 8, the safe speed vector set that the hydrogen fuel cell unmanned ship can reach within a certain time interval is called Reachable Avoidance Velocity (RAV) to represent with equation (23):

$$RAV = \{V \mid V \in RV, V \notin VO\} \quad (23)$$

C. MERGING THE EVALUATION FUNCTION OF THE DYNAMIC WINDOW METHOD

For the generated RAV, the fusion dynamic window method can generate the corresponding predicted trajectory for the speed combination (u_i, r_i) , and then evaluate the generated trajectory according to the designed evaluation function. In this section, in addition to selecting heading, speed, and distance as evaluation functions, and considering the constraints of COLREGS, a new rule constraint function is added to reflect the compliance degree of hydrogen fuel cell unmanned ship behavior to the rules. The evaluation function design is as follows:

(i) Heading evaluation function $heading(u, r)$

The heading evaluation function $heading(u, r)$ measures the degree to which the hydrogen fuel cell unmanned ship deviates from the target point. Introduce the angle error $\Delta\theta$ between the direction of the end position of the predicted

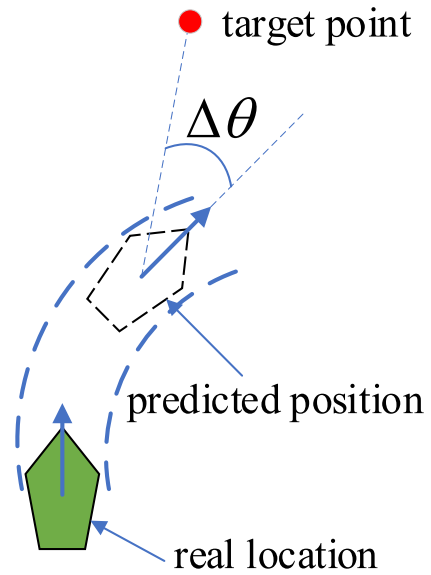


FIGURE 9. Schematic diagram of the angle between the predicted trajectory and the target.

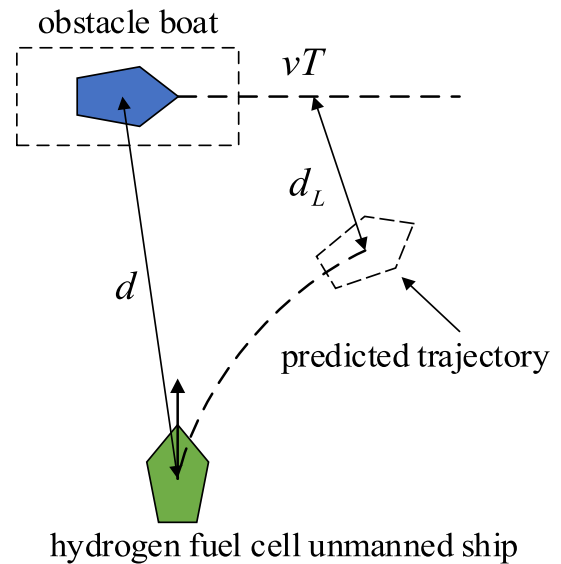


FIGURE 10. Principle of distance evaluation function.

trajectory and the line connecting the target point generated by the current speed combination, as shown in Figure 9. Considering that the hydrogen fuel cell unmanned ship should drive as straight as possible towards the target point, the greater the deviation of the trajectory heading angle, the lower the score of the evaluation function. The heading evaluation function can be designed as follows:

$$heading(u, r) = \pi - \Delta\theta \quad (24)$$

(ii) Velocity evaluation function $velocity(u, r)$

The speed evaluation function $velocity(u, r)$ measures the speed of the hydrogen fuel cell unmanned ship. Under the condition of ensuring safety, considering that the hydrogen

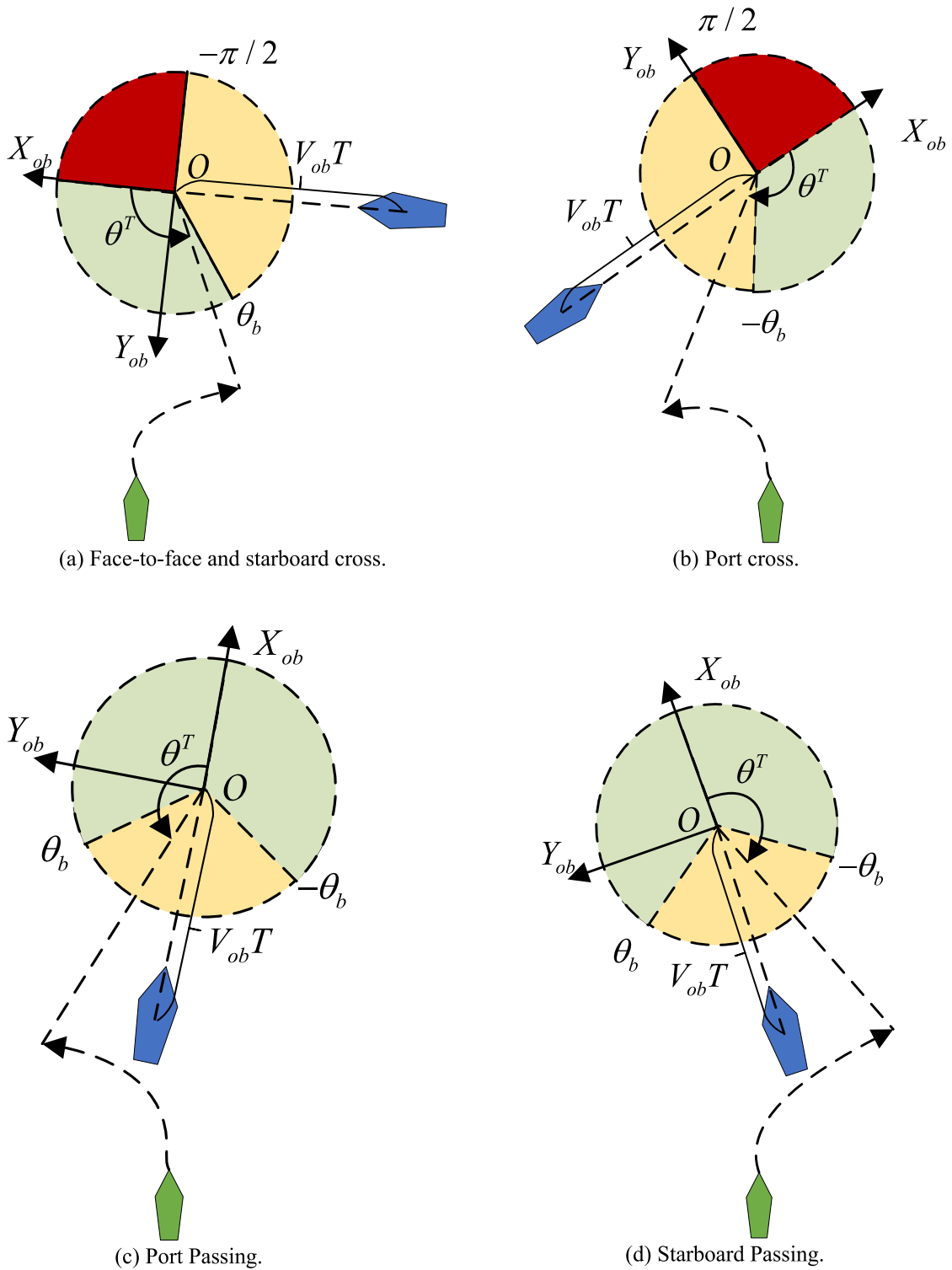


FIGURE 11. Schematic diagram of the principle of rule evaluation function.

fuel cell unmanned ship needs to reach the target point as soon as possible, so the higher the speed, the higher the evaluation function score. The speed evaluation function can be designed as follows:

$$velocity(u, r) = |u| \quad (25)$$

(iii) Distance evaluation function $dist(u, r)$

The distance evaluation function $dist(u, r)$ measures the distance between the obstacle ship and the hydrogen fuel cell unmanned ship. The farther the distance is, the higher the evaluation value is, the more inclined the hydrogen fuel cell unmanned ship is to choose this possible trajectory.

The principle of the distance evaluation function is shown in Figure 10.

In Figure 10, T represents the prediction time, and d represents the relative distance $L \in \{1, 2, \dots, T/dt\}$ between the two prediction trajectories at the predicted L -th moment. If the predicted trajectory of the hydrogen fuel cell unmanned ship enters the safety domain d_{save} of the obstacle ship, the evaluation value of the distance evaluation function is zero; if the predicted trajectory of the hydrogen fuel cell unmanned ship does not enter the safety domain of the obstacle ship, the value The shortest distance is used as the function value; if the distance between the hydrogen fuel cell unmanned ship and the obstacle is greater than a threshold d_{max} , the function value is set to a larger constant value. The distance evaluation function can be designed as follows:

$$dist(u, r) = \begin{cases} 0, & \min(d_L) < d_{save} \\ \min(d_L), & otherwise \\ N, & \min(d_L) > d_{max} \end{cases} \quad (26)$$

(iv) Added rule constraint function $colregs(u, r)$

When the hydrogen fuel cell unmanned ship performs the behavior of avoiding obstacle ships, it should comply with the constraints of maritime collision avoidance rules. However, in the evaluation function of the dynamic window method, there is no corresponding regulation on how the hydrogen fuel cell unmanned ship avoids obstacles. Therefore, the rule constraint function $colregs(u, r)$ is introduced. The predicted trajectory is evaluated, which represents the compliance degree of the collision avoidance behavior of the hydrogen fuel cell unmanned ship to the constraints of maritime regulations. Considering that the greater the avoidance range of the hydrogen fuel cell unmanned ship, the easier it is to complete the collision avoidance behavior, so it is less likely to affect the navigation of the obstacle ship, so the end of the predicted trajectory for the hydrogen fuel cell unmanned ship is opposite to the obstacle ship. The location distribution is used to measure the degree of compliance with the collision avoidance rules.

As shown in Figures 11(a), (b), (c), and (d), assuming that the obstacle ship moves in a straight line at a uniform speed, a coordinate system $X_{ob}OY_{ob}$ is established at the end of the obstacle ship's trajectory, where θ^T represents the relative azimuth of the hydrogen fuel cell unmanned ship's trajectory end position to the obstacle ship, θ_b . The boundary threshold is usually set at 112.5° to prevent the hydrogen fuel cell unmanned ship from following the obstacle ship. The rule constraint function can be expressed as follows:

$$colregs(u, r) = G(C_i, \theta_i^T) \quad (27)$$

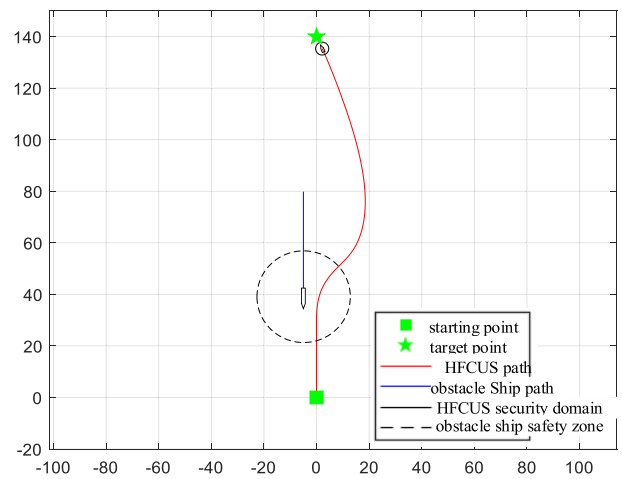
Among them, C_i represents the encounter situation between the hydrogen fuel cell unmanned ship and the obstacle ship, and the situations of encounter, left cross, left overtake, right overtake, and right cross are expressed as HO, CL, OTL, OTR, and CR, respectively. $G(\cdot)$ represents the evaluation

TABLE 1. Dynamic constraints of hydrogen fuel cell unmanned ships.

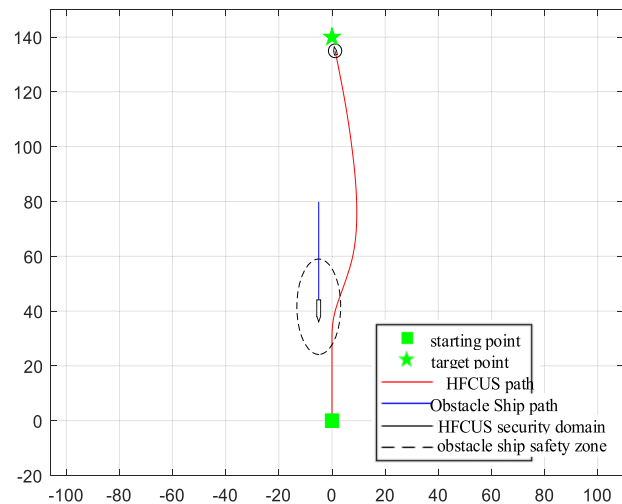
u_{min} (m/s)	u_{max} (m/s)	\dot{u} (m/s ²)	\dot{r} (°/s ²)	Velocity Resolution (m/s)	Angular Velocity Resolution (°/s)
0	4	1	20	0.01	1

TABLE 2. Specific parameters of fusion DWA algorithm.

Heading evaluati on Weight α	Distance evaluati on Weight β	Speed evaluati on Weight γ	Rule evaluati on Weight δ	Foreca st time T/s	Sampli ng time dt/s
0.5	0.2	0.3	0.45	0.5	0.1



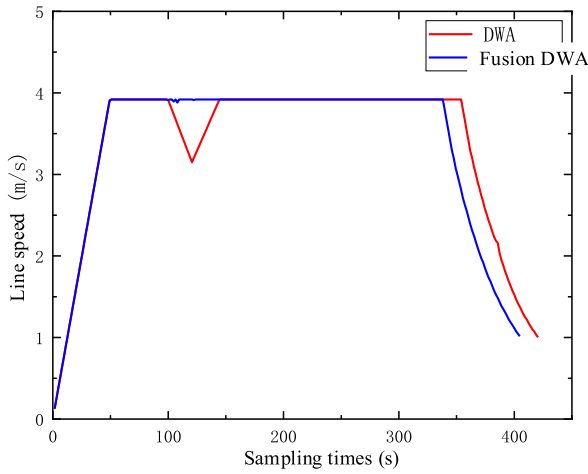
(a) Traditional DWA collision avoidance path.



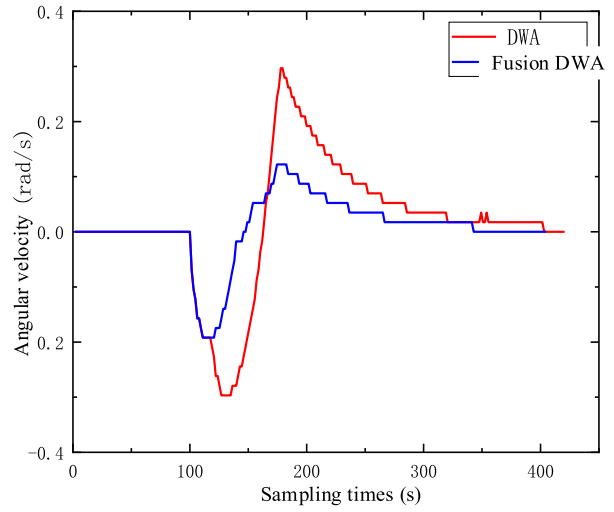
(b) Fusion DWA collision avoidance path.

FIGURE 12. Dynamic collision avoidance process in confrontation situation.

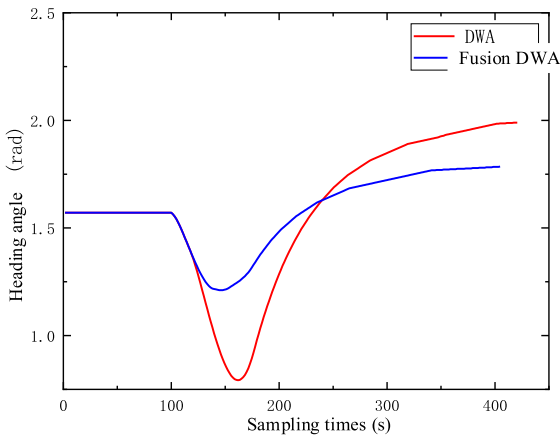
function of hydrogen fuel cell unmanned ship's compliance with maritime collision avoidance rules. According to the different encounter situations C_i between hydrogen fuel cell unmanned ship and obstacle ship, $G(\cdot)$ can be divided into



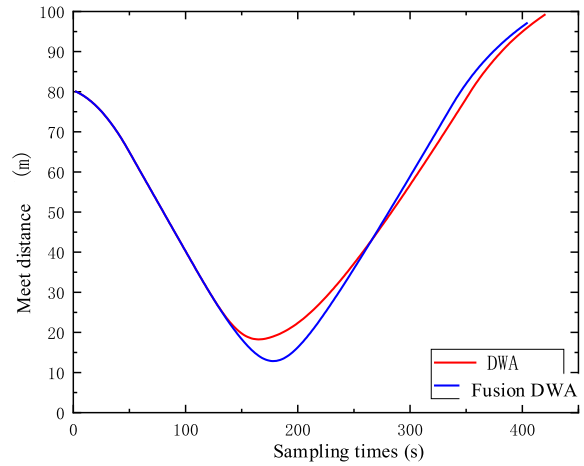
(a) Linear speed of hydrogen fuel cell unmanned ship.



(b) Angular velocity diagram of hydrogen fuel cell unmanned ship.



(c) Heading angle of hydrogen fuel cell unmanned ship.



(d) The meeting distance between two ships.

FIGURE 13. Comparison of collision avoidance curves of two algorithms.

four parts, as follows: The equation shows:

$$G(C_i, \theta_i^T) = \begin{cases} G_1(\cdot), & C_i = HO \text{ or } CR \\ G_2(\cdot), & C_i = CL \\ G_3(\cdot), & C_i = OTR \\ G_4(\cdot), & C_i = OTL \end{cases} \quad (28)$$

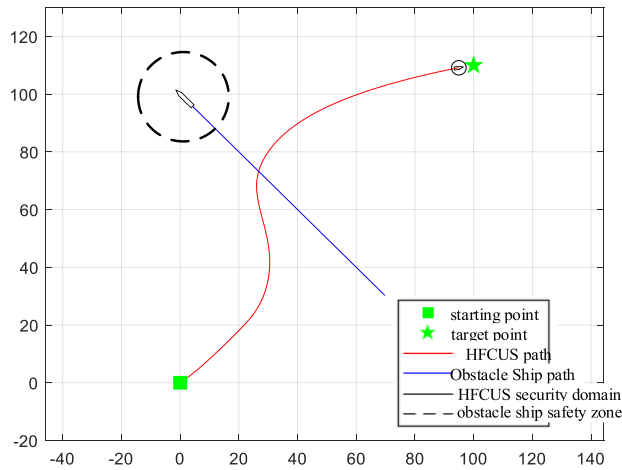
When the hydrogen fuel cell unmanned ship meets the obstacle ship and presents a right cross or confrontation, the hydrogen fuel cell unmanned ship needs to consider passing behind the port side of the obstacle ship without hindering the current navigation of the obstacle ship. The manned ship needs to actively turn to its starboard side to complete the collision avoidance behavior. At this time, the rule constraint function $G_1(\cdot)$ is considered:

$$G_1(C_i, \theta_i^T) = \begin{cases} |\theta_i^T|, & 0 \leq \theta_i^T < \theta_{th} \\ 0, & -\pi/2 < \theta_i^T \leq 0 \\ \theta_{th}, & \text{else} \end{cases} \quad (29)$$

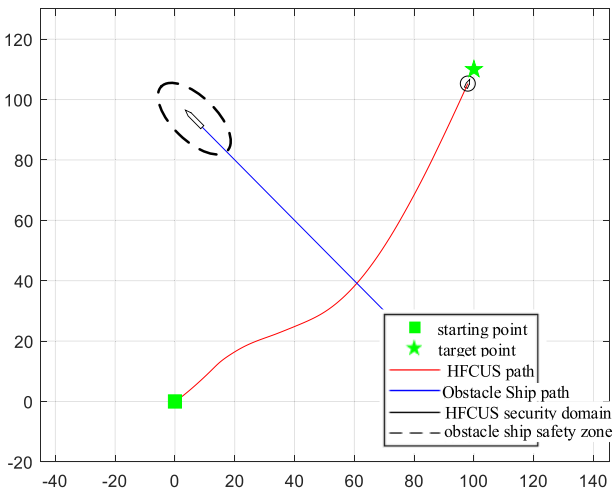
When the hydrogen fuel cell unmanned ship meets the obstacle ship and presents a left cross, the hydrogen fuel cell unmanned ship needs to consider passing behind the starboard side of the obstacle ship without hindering the current navigation of the obstacle ship. It is necessary to actively turn to its own port to complete the collision avoidance behavior. At this time, the rule constraint function $G_2(\cdot)$ is considered:

$$G_2(C_i, \theta_i^T) = \begin{cases} |\theta_i^T|, & -\theta_{th} \leq \theta_i^T < 0 \\ 0, & 0 \leq \theta_i^T < \pi/2 \\ \theta_{th}, & \text{else} \end{cases} \quad (30)$$

When the hydrogen fuel cell unmanned ship meets the obstacle ship and presents a right overtaking situation, the hydrogen fuel cell unmanned ship needs to actively turn to its own starboard, quickly bypass the obstacle ship from the rear side of the obstacle ship, and consider the rules at this



(a) Traditional DWA collision avoidance path.



(b) Fusion DWA collision avoidance path.

FIGURE 14. Dynamic collision avoidance process in confrontation situation.

time function $G_3(\cdot)$:

$$G_3(C_i, \theta_i^T) = \begin{cases} \pi - |\theta_i^T|, & -\pi < \theta_i^T \leq -\theta_b \\ \pi - \theta_b, & \theta_i^T > -\theta_b \\ 0, & \text{else} \end{cases} \quad (31)$$

When the hydrogen fuel cell unmanned ship meets the obstacle ship and presents a left overtaking situation, the hydrogen fuel cell unmanned ship needs to actively turn to its own port, and quickly bypass the obstacle ship from the rear side of the obstacle ship. At this time, consider the rule constraints function $G_4(\cdot)$:

$$G_4(C_i, \theta_i^T) = \begin{cases} \pi - |\theta_i^T|, & \theta_b \leq \theta_i^T < \pi \\ \pi - \theta_b, & \theta_i^T < \theta_b \\ 0, & \text{else} \end{cases} \quad (32)$$

Combining the above four types of evaluation functions, the target evaluation function for each trajectory can be obtained

as follows:

$$M(u, r) = \sigma \left(\alpha \cdot \text{heading}(u, r) + \beta \cdot \text{dist}(u, r) + \gamma \cdot \text{velocity}(u, r) + \delta \cdot \text{colregs}(u, r) \right) \quad (33)$$

From the analysis of the evaluation functions above, it can be seen that the physical quantity units of each evaluation function are different, so they cannot be added directly when calculating the target evaluation function, so each evaluation function is normalized, which means normalization, and the normalization. The normalized values are multiplied by the corresponding weights and the total target evaluation function is calculated. The normalized operation equations are shown from equation (34) to equation (37):

$$\begin{aligned} \sigma \cdot \text{heading}(u, r) &= \text{normalize} - \text{heading}(i) \\ &= \frac{\text{heading}(i)}{\sum_{i=1}^n \text{heading}(i)} \end{aligned} \quad (34)$$

$$\begin{aligned} \sigma \cdot \text{velocity}(u, r) &= \text{normalize} - \text{velocity}(i) \\ &= \frac{\text{velocity}(i)}{\sum_{i=1}^n \text{velocity}(i)} \end{aligned} \quad (35)$$

$$\begin{aligned} \sigma \cdot \text{dist}(u, r) &= \text{normalize} - \text{dist}(i) \\ &= \frac{\text{dist}(i)}{\sum_{i=1}^n \text{dist}(i)} \end{aligned} \quad (36)$$

$$\begin{aligned} \sigma \cdot \text{colregs}(u, r) &= \text{normalize} - \text{colregs}(i) \\ &= \frac{\text{colregs}(i)}{\sum_{i=1}^n \text{colregs}(i)} \end{aligned} \quad (37)$$

In the equations, i represents the i -th predicted trajectory, and n is the total number of all sampled trajectories satisfying the constraints.

In the process of collision avoidance, the surface hydrogen fuel cell unmanned ship can obtain the collision avoidance reachable speed set RAV according to the algorithm requirements, and calculate the predicted trajectory corresponding to each speed combination (u, r) in RAV, through The trajectory target evaluation function obtains the velocity combination $\{(u, r) | M(u, r) \max\}$ with the highest evaluation value in the velocity space as the velocity combination at the next moment of the hydrogen fuel cell unmanned ship movement, so that Realize the behavior of the hydrogen fuel cell unmanned ship avoiding collision and moving to the target point.

IV. DYNAMIC COLLISION AVOIDANCE SIMULATION AND RESULT ANALYSIS AND VERIFICATION

In order to verify that the proposed collision avoidance method has better performance than the traditional dynamic window method, this section combines the three typical encounter situations stipulated in the COLREGS Convention to analyze the different encounter situations of traditional DWA and fusion DWA in hydrogen fuel cell unmanned ships. The comparison simulation is carried out in the obstacle ship scene. The length of the hydrogen fuel cell unmanned ship is 2m, and the radius R_A of the hydrogen fuel cell unmanned ship's circular safe area after expansion is 1.5m;

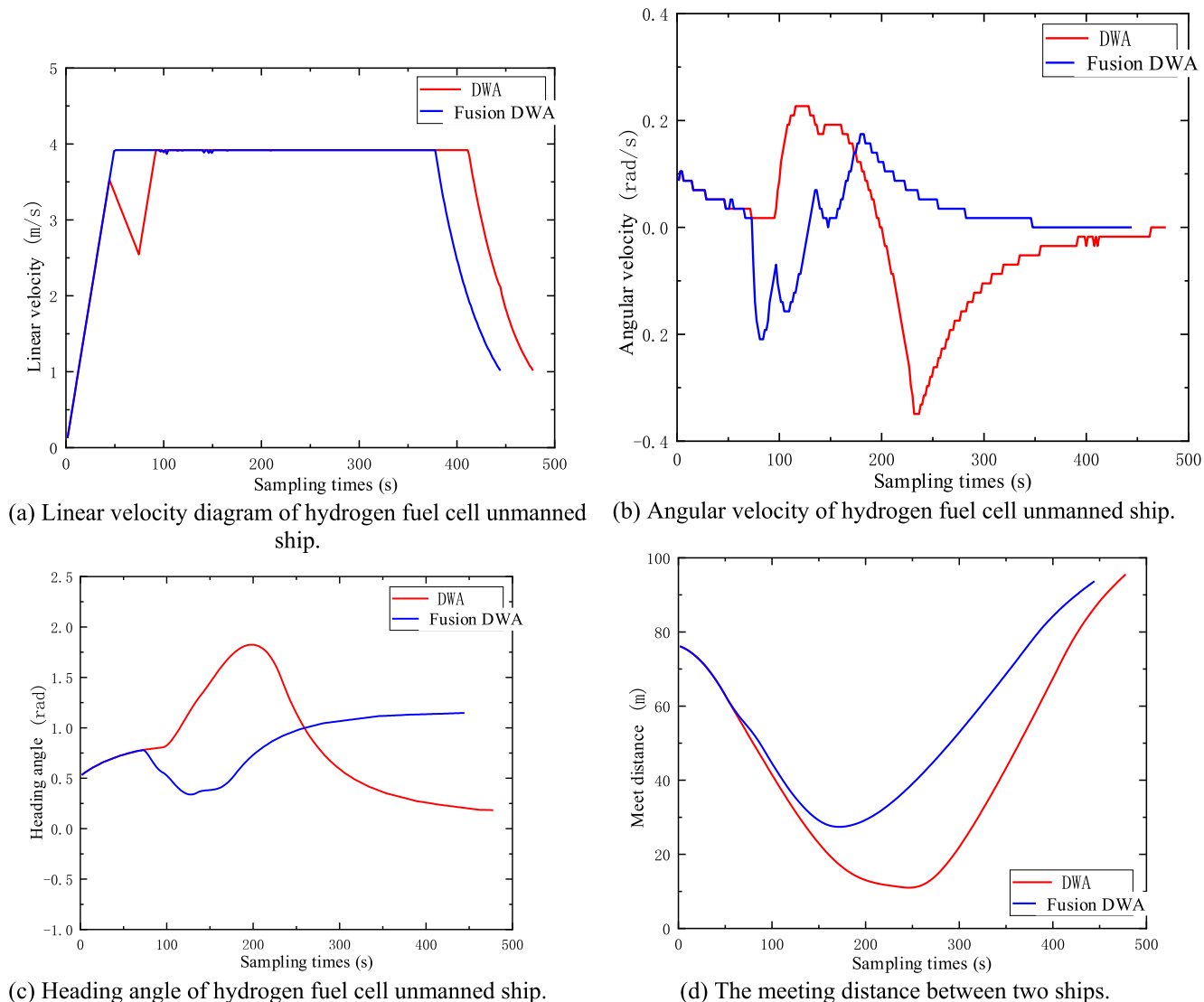


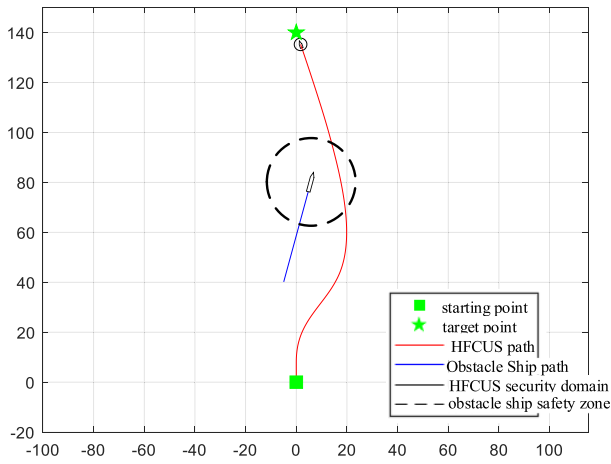
FIGURE 15. Comparison of collision avoidance curves of two algorithms.

the length of the obstacle ship is 6m, and the width of the ship is 2m. In order to leave enough space to meet the change of course and speed of the ship's collision avoidance behavior, the safety domain model of the obstacle ship is introduced, in which, the long and short semi-axes of the ellipse model are 2.5 times length and 1 times length of the ship, respectively. The basic parameters of the hydrogen fuel cell unmanned ship dynamics parameters and fusion DWA algorithm are shown in Table 1 and Table 2.

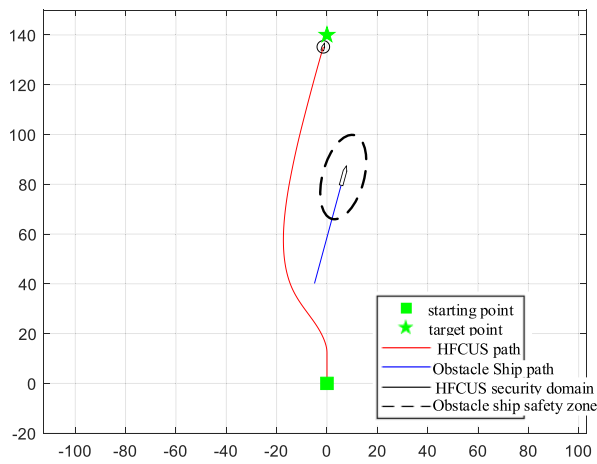
(i). Counter situation analysis

Set the starting point position of the hydrogen fuel cell unmanned ship as $[0m, 0m]$, the initial heading angle as $\pi/2$, the initial speed as $[0m/s, 0m/s, 0rad/s]$, and the target point position as $[0m, 140m]$. At the same time, a moving obstacle boat starts from the starting point $[-5m, 80m]$ and moves along the course of $-\pi/2$ at a speed of $1m/s$. Combined with the analysis of the COLREGS Convention, the hydrogen

fuel cell unmanned ship and the obstacle ship form a confrontation situation, and the hydrogen fuel cell unmanned ship needs to perform collision avoidance behavior to avoid the obstacle ship. The collision avoidance simulation of the two collision avoidance algorithms in the confrontation situation is shown in Figures 12(a), and (b). According to the constraints of the COLREGS Convention, the hydrogen fuel cell unmanned ship needs to turn to the starboard side to avoid the obstacle ship. The collision avoidance trajectories of the two algorithms in the figure all pass the port side of the obstacle ship, which meet the requirements of the rules. However, in the traditional DWA algorithm, the obstacle ship collision model is regarded as a safety circle, while the fusion DWA algorithm adopts the safety domain model, which retains more feasible paths for hydrogen fuel cell unmanned ships, and one obtains a better collision avoidance path is obtained.



(a) Traditional DWA collision avoidance path.



(b) Fusion DWA collision avoidance path.

FIGURE 16. Dynamic collision avoidance process in overtaking situation.

Figures 13(a) and (b) respectively represent the change diagrams of the speed and angular velocity of the hydrogen fuel cell unmanned ship under the two algorithms. Under the action of the velocity evaluation function $velocity(u, r)$, the hydrogen fuel cell unmanned ship quickly accelerates to the maximum speed $u = 4m/s$ to sail, under the traditional DWA algorithm, the hydrogen fuel cell unmanned ship encounters an obstacle ship, and avoids collision by combining large speed reduction and large angular velocity transformation, while the fusion DWA has certain predictability, and chooses a better collision avoidance. The trajectory, speed and angular velocity change curves also have smaller changes, which is more in line with the mechanical properties of hydrogen fuel cell unmanned ship motion. Figure 13(c) represents the course diagram of the hydrogen fuel cell unmanned ship. It can be seen that the collision avoidance course acquired by the fusion of DWA is smoother, and the course change is smaller, which is conducive to the safe navigation of the hydrogen fuel cell unmanned ship. Figure 13(d) represents the distance between the hydrogen

fuel cell unmanned ship and the obstacle ship, where the obstacle model in the safety domain used in the integration of DWA, the shortest distance is greater than the short axis length of the safety domain model, successfully obtained under the premise of safe collision avoidance. Better collision avoidance path, shorter collision avoidance path and less time-consuming.

(ii). Cross Situation Analysis

Set the initial position of the hydrogen fuel cell unmanned ship to $[0m, 0m]$, the initial heading angle to $\pi/6$, the initial speed to $[0m/s, 0m/s, 0rad/s]$, and the target point position to $[100m, 110m]$. At the same time, a moving obstacle boat starts from the starting point $[70m, 30m]$ and moves along a course of $3\pi/4$ at a speed of $2m/s$. Combined with the analysis of the COLREGS Convention, the hydrogen fuel cell unmanned ship and the obstacle ship constitute the starboard crossing situation in the crossing situation. The hydrogen fuel cell unmanned ship needs to turn to the starboard to avoid the obstacle ship, and it avoids the obstacle ship from the rear side without hindering the obstacle ship sailing. The collision avoidance simulation of the two collision avoidance algorithms in the encounter situation is shown in Figures 14(a), and (b). It can be seen from the figure that the fusion DWA is affected by the rule constraint function $colregs(u, r)$, and turns to avoid from the starboard side as required, and passes behind the obstacle ship to reach the target point, while the traditional DWA lacks rule constraints and turns to the port side passing in front of the obstacle boat affects the navigation of the obstacle boat and increases the risk of collision, and follows the obstacle boat until it bypasses the bow of the obstacle boat, prolonging the collision avoidance path.

Figures 15(a) and (b) represent the change diagrams of the speed and angular velocity of the hydrogen fuel cell unmanned ship, respectively. Under the traditional DWA algorithm, the hydrogen fuel cell unmanned ship encounters an obstacle ship, and the speed is greatly reduced to prevent collision with the obstacle ship. The bow of the obstacle ship passes by, the hydrogen fuel cell unmanned ship accelerates to the maximum speed until it bypasses the obstacle ship, and the fusion DWA algorithm adds the rule constraint function $colregs(u, r)$, the hydrogen fuel cell unmanned ship drives from the stern. However, the speed changes smoothly, the angular velocity adjustment range is smaller, and the navigation process is more stable. Figure 15(c) represents the movement course diagram of the hydrogen fuel cell unmanned ship. It can be seen that the collision avoidance course of the integrated DWA changes less, which is conducive to the safe navigation of the hydrogen fuel cell unmanned ship. Figure 15(d) represents the distance between the hydrogen fuel cell unmanned ship and the obstacle ship, where the hydrogen fuel cell unmanned ship passed in front of the obstacle ship under traditional DWA, and the hydrogen fuel cell unmanned ship invaded the safe zone of the obstacle ship. This greatly increases the collision risk of the hydrogen

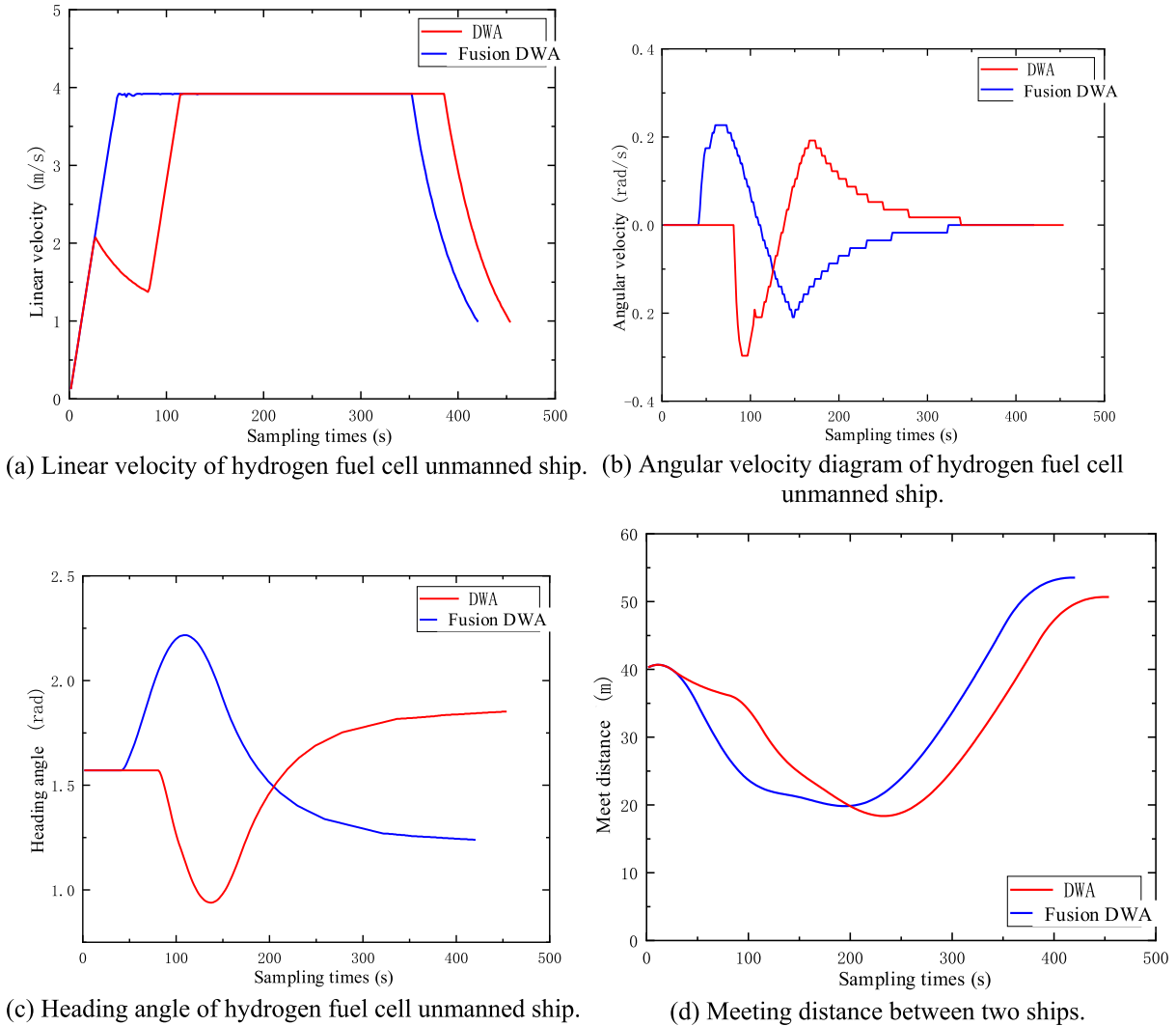


FIGURE 17. Comparison of collision avoidance curves of two algorithms.

TABLE 3. Motion parameters of obstacle boat.

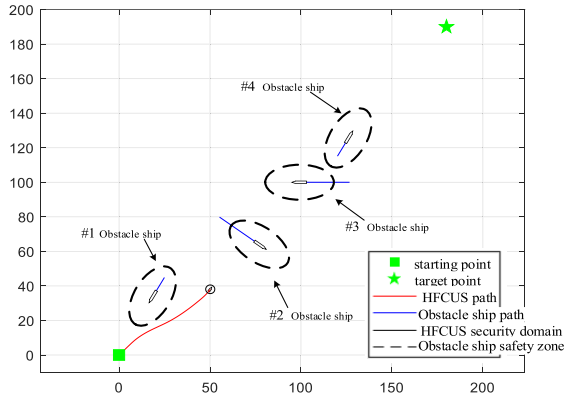
Obstacle boat	Starting point(m)	Speed(m/s)	Heading(rad)
#1	(25,45)	0.75	$-2\pi/3$
#2	(55,80)	1.5	$-\pi/5$
#3	(127,100)	1.5	π
#4	(120,115)	0.75	$\pi/3$

fuel cell unmanned ship, while the fusion DWA chooses to pass behind the obstacle ship, which has a larger shortest encounter distance and higher safety.

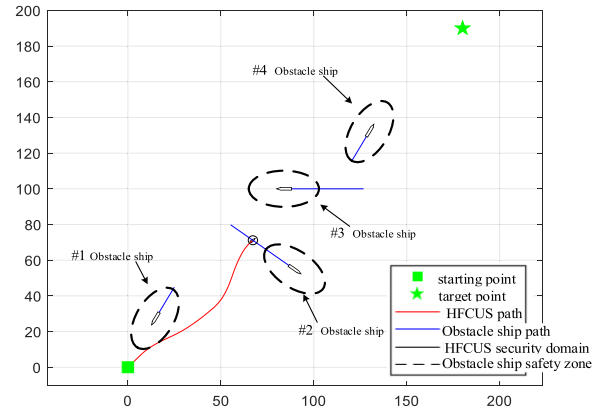
(iii). Overtaking Situation Analysis

Set the initial position of the hydrogen fuel cell unmanned ship to $[0m, 0m]$, the initial heading angle to $\pi/2$, the initial speed to $[0m/s, 0m/s, 0rad/s]$, and the target point position to $[0m, 140m]$. At the same time, a moving obstacle boat starts from the starting point $[-5m, 40m]$ and moves along a course of $5\pi/12$ at a speed of $1m/s$. Combined with the analysis of the COLREGS Convention, the hydrogen fuel

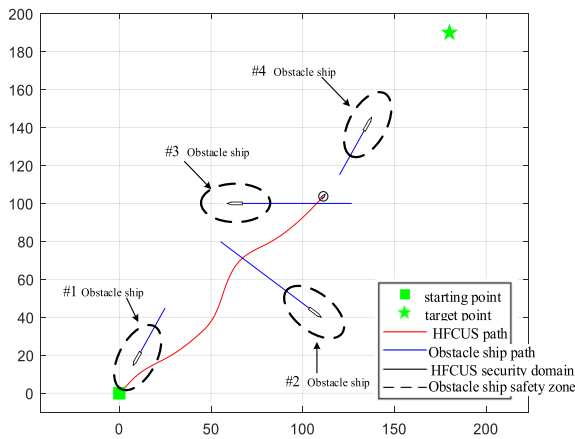
cell unmanned ship and the obstacle ship constitute the port overtaking situation in the overtaking situation. The hydrogen fuel cell unmanned ship need to turn to the port side to avoid the obstacle ship, and dodge from the rear side of the obstacle ship without hindering it. Obstacles to the navigation of the ship. The collision avoidance simulation of the two collision avoidance algorithms in the confrontation situation is shown in Figures 16(a), and (b). It can be seen from the figure that the fusion DWA is affected by the rule constraint function $colregs(u, r)$, and turns to avoid from the port side as required, and passes behind the obstacle ship to reach the target point,



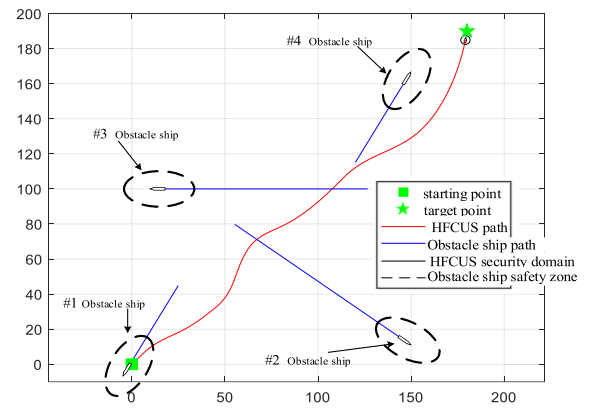
(a) Hydrogen fuel cell unmanned ship first meets obstacle ship No.1.



(b) Hydrogen fuel cell unmanned ship meets obstacle ship No.2.



(c). Hydrogen fuel cell unmanned ship meets obstacle ship No. 3.



(d). Hydrogen fuel cell unmanned ship meets obstacle ship No. 4.

FIGURE 18. Simulation diagram of multi-vessel collision avoidance.

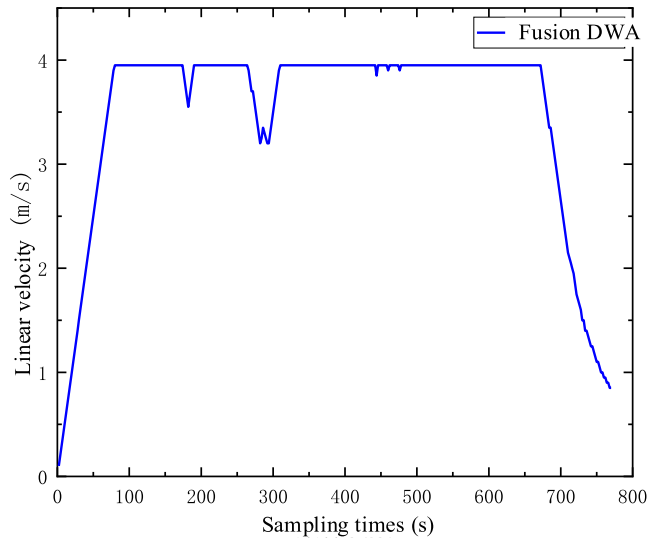
while the traditional DWA lacks rule constraints and turns to the starboard side. Passing in front of the obstacle boat affects the navigation of the obstacle boat and increases the risk of collision.

Figures 17(a) and (b) represent the changes of the speed and angular velocity of the hydrogen fuel cell unmanned ship, respectively. Under the traditional DWA algorithm, the hydrogen fuel cell unmanned ship executes the avoidance time later, so by greatly reducing the speed and greatly adjusting the angular velocity to meet the requirements of collision avoidance, and the fusion DWA algorithm adds the rule constraint function $colregs(u, r)$, the hydrogen fuel cell unmanned ship passes by the stern, the speed changes smoothly, and the movement of the obstacle ship is predicted in advance, making the hydrogen fuel cell unmanned ship more efficient. Early evasive action makes the navigation process more stable. Figure 17(c) represents the movement course diagram of the hydrogen fuel cell unmanned ship. It can be seen that the collision avoidance course of the integrated DWA changes less, which is conducive to the

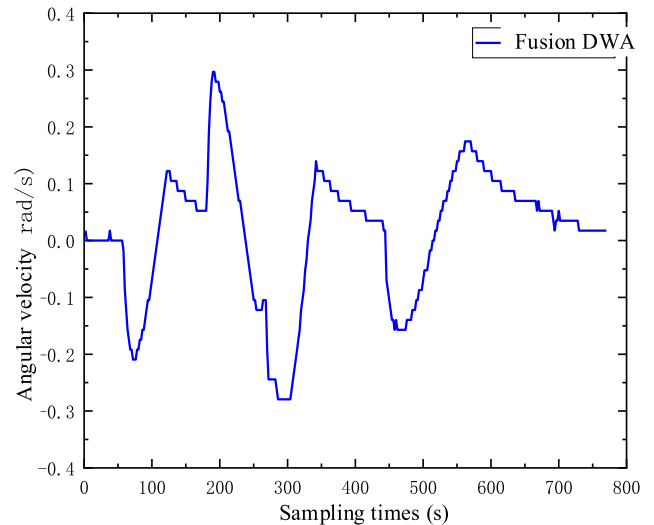
safe navigation of the hydrogen fuel cell unmanned ship. Figure 17(d) represents the distance between the hydrogen fuel cell unmanned ship and the obstacle ship, where the hydrogen fuel cell unmanned ship passes in front of the obstacle ship under the traditional DWA, and the closest encounter distance is smaller, and the hydrogen fuel cell unmanned ship is added. The collision risk of the ship, while the fusion DWA chooses to pass behind the obstacle ship, which has a larger closest encounter distance and higher safety.

(iv). Multi-ship encounter situation

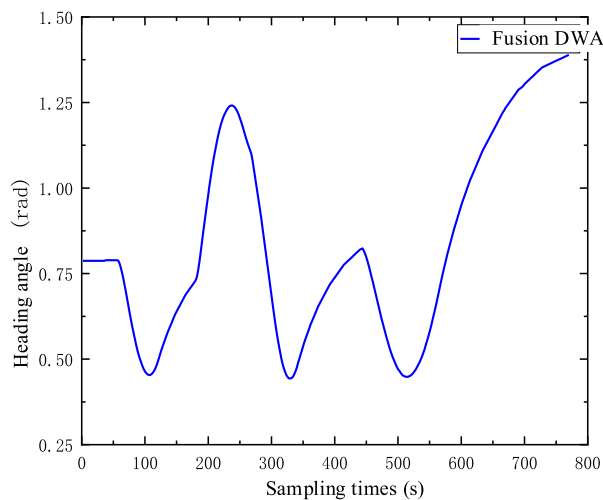
Considering the collision avoidance simulation of the hydrogen fuel cell unmanned ship in the presence of multi-obstacle ships. Among them, the initial position of the hydrogen fuel cell unmanned ship is set to $[0m, 0m]$, the initial heading angle is $\pi/4$, the initial speed is $[0m/s, 0m/s, 0rad/s]$, and the target point position is $[0m, 140m]$. The motion parameters of the obstacle boat are shown in Table 3. The hydrogen fuel cell unmanned ship moves from the starting point to the target point, and it avoids the obstacle ship that has the risk of collision during



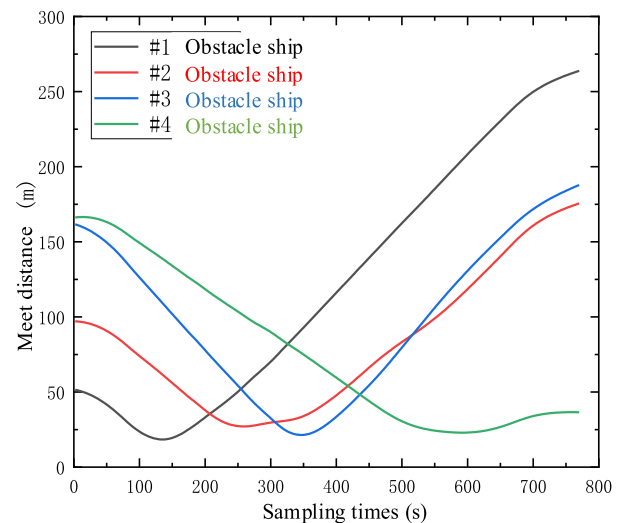
(a) Linear velocity of hydrogen fuel cell unmanned ship.



(b) Angular velocity of hydrogen fuel cell unmanned ship.



(c) Heading angle of hydrogen fuel cell unmanned ship.



(d) Meeting distance between two ships.

FIGURE 19. Schematic diagram of algorithm collision avoidance curve.

the voyage. The schematic diagram of collision avoidance simulation is shown in Figures 18(a), (b), (c) and (d).

In Figure 18(a), the hydrogen fuel cell unmanned ship first meets the obstacle ship #1, which constitutes the confrontation situation in the COLREGS convention. At this time, under the action of the rule evaluation function, the hydrogen fuel cell unmanned ship chooses to turn to starboard dodge. In Figure 18(b), the hydrogen fuel cell unmanned ship encounters obstacle ship #2, forming a left crossing situation. At this time, the hydrogen fuel cell unmanned ship turns to the port side and passes the stern of the obstacle ship without affecting the obstacle ship sailing. In Fig. 18(c), the hydrogen fuel cell unmanned ship and the obstacle ship #3 form a right crossing situation, and the hydrogen fuel cell unmanned ship turns to the starboard side to perform avoidance and passes by the stern of the obstacle ship.

In Figure 18(d), the hydrogen fuel cell unmanned ship and the obstacle ship form a starboard overtaking situation, and the hydrogen fuel cell unmanned ship turns to the starboard direction, surpasses the obstacle ship #4 and reaches the target point. Figures 19(a), (b), (c) and (d) are the collision avoidance curve of the hydrogen fuel cell unmanned ship during its navigation. The results show that the hydrogen fuel cell unmanned ship can maintain the maximum speed during the whole navigation process, the change of the angular velocity is relatively gentle, and the change of the course is relatively smooth. The closest encounter distances between them are all greater than the safety threshold, and the constraints of the COLREGS convention are strictly followed during the navigation process to ensure the safety of navigation, which reflects the effectiveness of the proposed fusion DWA algorithm for the multi-vessel collision avoidance process.

V. CONCLUSION

This study first analyzes the basic principles of the speed obstacle theory and introduces the ship safety field to improve the speed obstacle set, so that the avoidance behavior of hydrogen fuel cell unmanned ship can retain more feasible paths. On this basis, the improved speed obstacle set is introduced into the discrete speed window, and the speed vector is screened to realize the fusion of algorithms. Finally, the evaluation function is improved, and the rule evaluation function constraint function is introduced, so that the avoidance behavior of the hydrogen fuel cell unmanned ship to the dynamic obstacle ship conforms to the constraints of the COLREGS convention, and the safety in the process of collision avoidance is improved. Finally, the fusion DWA algorithm and the traditional DWA algorithm are applied to three typical encounter situations for analysis. Through comparison and simulation, the results show that the fusion DWA can effectively avoid the dynamic obstacle ship, and the avoidance behavior obeys the constraints of the rules, and has a better course and speed performance; in addition, the fusion DWA algorithm is applied to the simulation in the presence of multiple ships, and the results show that the proposed algorithm can also effectively avoid dynamic obstacle ships in the case of multiple ships, and the avoidance behavior conforms to the constraints of the rules, and have a good performance security.

REFERENCES

- [1] D. Çalisir, S. Ekici, A. Midilli, and T. H. Karakoc, "Benchmarking environmental impacts of power groups used in a designed UAV: Hybrid hydrogen fuel cell system versus lithium-polymer battery drive system," *Energy*, vol. 262, Jan. 2023, Art. no. 125543.
- [2] C.-C. Lin and C.-C. Hsieh, "Study on proton exchange membrane fuel cells performance design: A case study of a small surface boat," *Alexandria Eng. J.*, vol. 61, no. 6, pp. 4491–4505, Jun. 2022.
- [3] S. Mekhilef, R. Saidur, and A. Safari, "Comparative study of different fuel cell technologies," *Renew. Sustain. Energy Rev.*, vol. 16, no. 1, pp. 981–989, 2012.
- [4] G. De Lorenzo, F. Piraino, F. Longo, G. Tinè, V. Boscaino, N. Panzavecchia, M. Caccia, and P. Fragiaco, "Modelling and performance analysis of an autonomous marine vehicle powered by a fuel cell hybrid powertrain," *Energies*, vol. 15, no. 19, p. 6926, Sep. 2022, doi: 10.3390/en15196926.
- [5] F. H. Bagherian, M. R. Firozjaee, A. M. Mir, and R. Youneszadeh, "Fuel cell power system conceptual design for unmanned underwater vehicle," *Hydrogen, Fuel Cell Energy Storage*, vol. 10, no. 1, pp. 33–50, 2023.
- [6] T. Vairo, D. Cademartori, D. Clematis, M. P. Carpanese, and B. Fabiano, "Solid oxide fuel cells for shipping: A machine learning model for early detection of hazardous system deviations," *Process Saf. Environ. Protection*, vol. 172, pp. 184–194, Apr. 2023.
- [7] A. M. Bassam, A. B. Phillips, S. R. Turnock, and P. A. Wilson, "An improved energy management strategy for a hybrid fuel cell/battery passenger vessel," *Int. J. Hydrogen Energy*, vol. 41, no. 47, pp. 22453–22464, Dec. 2016.
- [8] F. Li, Y. Yuan, X. Yan, R. Malekian, and Z. Li, "A study on a numerical simulation of the leakage and diffusion of hydrogen in a fuel cell ship," *Renew. Sustain. Energy Rev.*, vol. 97, pp. 177–185, Dec. 2018.
- [9] W. Guan, J. Chen, L. Chen, J. Cao, and H. Fan, "Safe design of a hydrogen-powered ship: CFD simulation on hydrogen leakage in the fuel cell room," *J. Mar. Sci. Eng.*, vol. 11, no. 3, p. 651, Mar. 2023, doi: 10.3390/jmse11030651.
- [10] Y. Song, Y. Chen, J. Gao, Y. Wang, and G. Pan, "Collision avoidance strategy for unmanned surface vessel considering actuator faults using kinodynamic rapidly exploring random tree-smart and radial basis function neural network-based model predictive control," *J. Mar. Sci. Eng.*, vol. 11, no. 6, p. 1107, May 2023, doi: 10.3390/jmse11061107.
- [11] Z. Zhu, Y. Yin, and H. Lyu, "Automatic collision avoidance algorithm based on route-plan-guided artificial potential field method," *Ocean Eng.*, vol. 271, Mar. 2023, Art. no. 113737.
- [12] D. Xue, D. Wu, A. S. Yamashita, and Z. Li, "Proximal policy optimization with reciprocal velocity obstacle based collision avoidance path planning for multi-unmanned surface vehicles," *Ocean Eng.*, vol. 273, Apr. 2023, Art. no. 114005.
- [13] J. Tang, X. Chen, X. Zhu, and F. Zhu, "Dynamic reallocation model of multiple unmanned aerial vehicle tasks in emergent adjustment scenarios," *IEEE Trans. Aerosp. Electron. Syst.*, vol. 59, no. 2, pp. 1139–1155, Apr. 2023.
- [14] J. Tang, G. Liu, and Q. Pan, "A review on representative swarm intelligence algorithms for solving optimization problems: Applications and trends," *IEEE/CAA J. Autom. Sinica*, vol. 8, no. 10, pp. 1627–1643, Oct. 2021.

ZIMIN WANG was born in Wuhan, Hubei, China, in 2000. From 2019 to 2023, he was a Research Assistant with the International College, Wuhan University of Science and Technology, Wuhan. His research interests include the development of intelligent route optimization, ant colony algorithm, autonomous underwater vehicle, intelligent energy consumption, neural networks, and genetic algorithm.

• • •